ANALYSIS OF CONVENTIONAL AND FEM APPROACH TO UPSETTING 6061 ALUMINIUM CYLINDERS

Josip Cumin[1], Domagoj Flegar[1], Daniel Novoselović[1], Dejan Marić[1] , Waldemar Matysiak[2]

[1]*Mechanical engineering faculty in Slavonski Brod, University of Slavonski Brod*
[2]*Mechanical engineering faculty in Poznan, Poland*

Key words: *6061 aluminium, tool, cylinder, upsetting*

Abstract: This article shows comparison of theoretical and finite element method numerical solutions to 6061 aluminium cylinders upsetting. In the simple DOE, different heights of cylinders are specified to which aluminium cylinders are compressed. For the compressed state, the equivalent strain and equivalent stress were calculated and compared.

1 INTRODUCTION

The upsetting process is widely used in the bulk metal forming industry [1]. Furthermore, the upsetting process is vastly used in forging processes as the first stage where material is well deformed. Forging upsetting is performed in the hot material state [1-3].

Cold upsetting process is typically related to the material testing (determination of stress-strain relations). Cold upsetting is different by the physics of body contacts between tool and workpiece, by the means of high surface quality, good lubrication and low friction factor [4,5,6]. Barreling of the specimen (product) occurs due to the friction at the contact surfaces, which prevents particle movement and material flow at those surfaces (Figure 1).

Figure 2 shows material flow lines after cylinder upsetting. The higher is ratio h_0/h_1, the better is material flow. This leads to better mechanical properties by the means of better product ductility/toughness. For the first forging operation, upsetting ratio is defined as [3]:

$$m = \frac{h_0}{d_0} = \frac{h_0}{a_\square} = 1,5 \div 2,8 \tag{1}$$

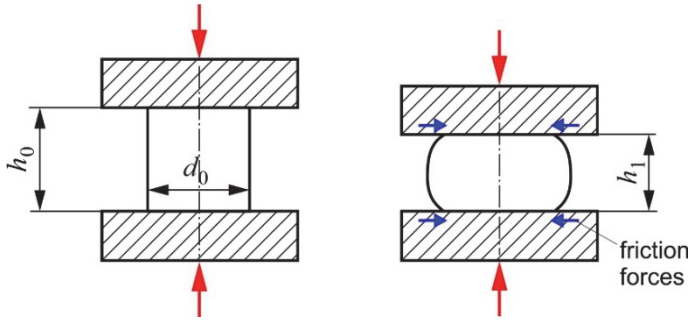

Figure 1. Friction forces on contact surfaces

Figure 2. Material flow lines in the deformed cylinder

During forming the material is under compression stresses (triaxial, after barreling), and true strain can be calculated [1-3] as:

$$\varphi = \ln\left(\frac{h_0}{h_1}\right) \tag{2}$$

For the case of uniaxial loading (without barreling effect) the true stress can be calculated as [3]:

$$k_f = \frac{F}{A},\ \text{MPa} \tag{3}$$

where F - loading force / N; A - current (true) surface of specimen/ mm^2

For the axisymmetric stress state consideration and slab theory, calculation of upsetting force is made by following expression [1]:

$$F_{KON} = A_1 \cdot k_f \left(1 + \frac{\mu}{3} \cdot \frac{d_1}{h_1}\right),\ \text{N} \tag{4}$$

where A_1 - current specimen surface / mm^2, k_f - true stress in material / MPa, μ - coefficient of friction (for cold upsetting and lubricated conditions $\mu = 0{,}05 \div 0{,}15$), d_1 - diameter of specimen at the end of upsetting / mm, h_1 - height of specimen at the end of upsetting / mm.

2 MATERIAL

For the material, an aluminium alloy EN AW-6060 was used. This material is also found as AlMgSi, BS EN 573-3:2009. Table 1 gives chemical composition of this alloy according to EN573-3 (EN AW-6060) [7-10]. Table 2 gives typical mechanical properties for the alloy [7-10].

Table 1. Chemical composition of EN AW-6060 / %

Si	Fe	Cu	Mn	Mg	Cr	Zn	Ti	Others	
								each	total
0,3÷0,6	0,1÷0,3	max. 0,1	max. 0,1	0,35÷0,6	max. 0,05	max. 0,15	max. 0,1	max. 0,05	max. 0,15

Table 2. Mechanical properties of EN AW-6060 alloy

Temper state	Thickness e / mm	Yield stress $R_{p0,2}$ / MPa	Tensile strength R_m /MPa	Elongation A / %	Hardness / HB
T4	≤25	60	120	16	45
T5	$5 < e \leq 25$	100	140	8	50
T6	$5 < e \leq 25$	140	170	8	60
T66	$5 < e \leq 25$	150	195	8	65

Where: T4-Naturally aged to a stable condition, T5-cooled from an elevated temperature forming operation and artificially aged, T6-Solution heat treated, quenched and artificially aged, T66-cooled from an elevated temperature forming operation and artificially aged to a condition with higher mechanical properties through special control of manufacturing processes [8].

For the finite element method (FEM), the mathematical model of true stress/true strain is needed. This was obtained from the material data book [10]:

$$k_f = M \cdot e^{m_1 \vartheta} \cdot \varphi^{m_2} \cdot e^{m_4/\varphi} \cdot \dot{\varphi}^{m_3},\ \text{MPa} \tag{5}$$

where:
m_1 - coefficient of temperature; $m_1 = -0{,}00128$
m_2 - coefficient of strain; $m_2 = 0{,}10762$
m_4 - coefficient of strain; $m_4 = -0{,}01430$
m_3 - coefficient of strain rate; $m_3 = -0{,}00766$
M - coefficient; $M = 242{,}066$

For the Msc.Marc finite element method software, the material data input needs to be in the form of a true stress as the function of equivalent plastic strain, so this was calculated as follows:

$$\varphi_{pl} = \varphi - \frac{k_f}{E} \tag{6}$$

3 FINITE ELEMENT METHOD

For the finite element method (FEM) two programs were used, Ansys (static, nonlinear analysis) and Msc.Marc. For the Ansys software, a 3D model was created in Autodesk Inventor and it was imported into Ansys, meshed with 8 node brick elements which have multilinear hardening model (piecewise linear) according to equation (5). Contact plates were modeled as cylinders with low alloy steel material properties (normalized AISI 4140 steel material model). Friction and contacts were managed automatically with defined friction coefficient of μ=0,1 (lubricated conditions) [1, 11].

Other material parameters were defined as:

-modulus of elasticity E = 69900 MPa

-density ρ = 2698,8 kg/m^3

-ambient temperature υ = 22 °C

- average strain rate $\dot{\varphi} = 0{,}055\ s^{-1}$

Lower tool was modeled as fixed, and upper tool as movable with variable upsetting heights. Variable upsetting heights with calculated analytical values are shown in table 3. Basic cylinder dimensions at the beginning of upsetting were defined as ϕ18 x 27 mm.

Table 3. Calculated analytical values from experiment upsetting heights

No:	Height h_1 / mm	φ	k_f / MPa	φ_{pl}	A_1 / mm^2	d_1 / mm	F / N
1.	25	0,077	151,63	0,075	274,83	18,71	43232,25
2.	23	0,16	180,75	0,158	298,72	19,50	56282,32
3.	21	0,251	195,93	0,249	327,17	20,41	67217,12
4.	19	0,351	206,44	0,348	361,61	21,46	78867,72
5.	17	0,462	214,73	0,460	404,16	22,68	92576,38

Figure 3 shows results for upsetting height of h_1 = 25 mm (Ansys).

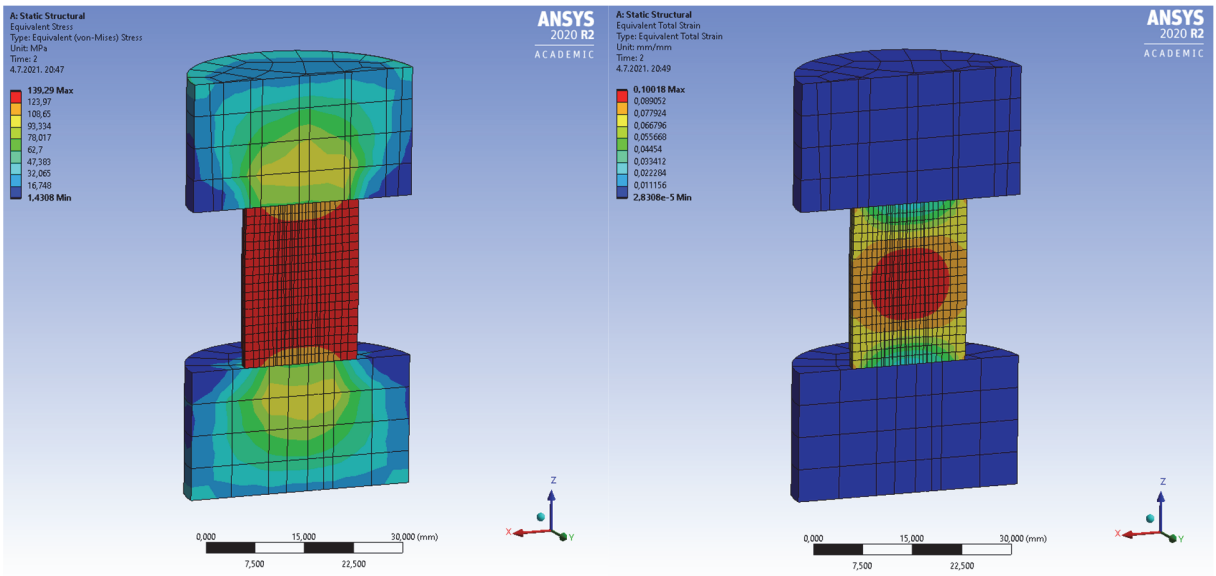

Figure 3. Von Mises stress and equivalent total strain for height of 25 mm

Figure 4 shows equivalent Von Mises stress and equivalent total strain for upsetting height of h_1 = 25 mm (Msc.Marc).

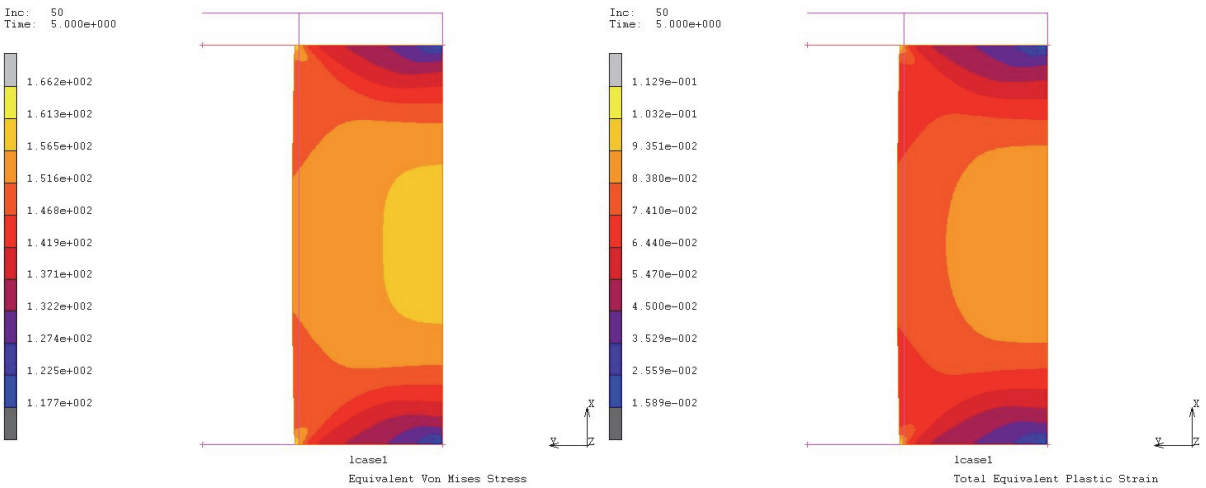

Figure 4. Von Mises stress and equivalent total strain for height of 25 mm

In Msc.Marc the cylinder was modeled as axisymmetric body, where main (symmetry) axis needs to be positioned in *x*-axis of the coordinate system [12]. For the analysis, a 4 node isoparametric axisymmetric element 10 was used. It has 4 integration points (full integration, updated Lagrange method and additive decomposition, large strain in the first case); and full integration with multiplicative decomposition in the second case.

Lower tool was modeled as fully constrained rigid body, upper as movable rigid body with displacements as per table 3. Contacts were defined through CTABLE option, with displacement related solving method and friction coefficient of μ=0,1 [1, 11].

Figure 5 shows results for upsetting height of h_1 = 23 mm (Ansys).

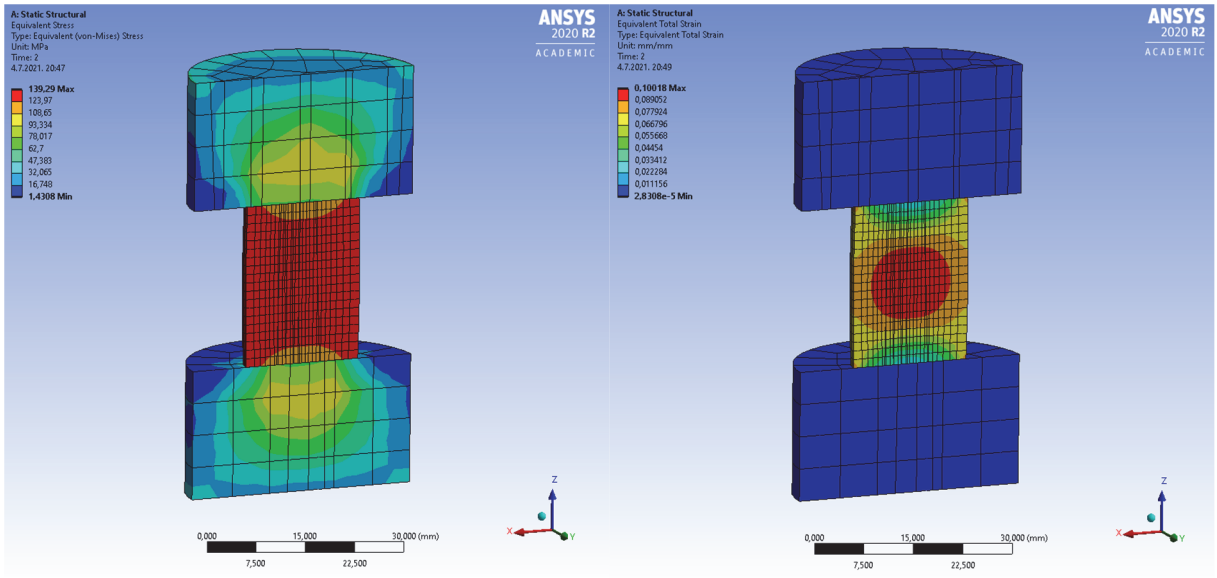

Figure 5. Von Mises stress and equivalent total strain for height of 25 mm

Figure 6 shows equivalent Von Mises stress and equivalent total strain for upsetting height of h_1 = 23 mm (Msc.Marc).

Figure 7 shows results for upsetting height of h_1 = 21 mm (Ansys).

Figure 8 shows equivalent Von Mises stress and equivalent total strain for upsetting height of h_1 = 21 mm (Msc.Marc).

Figure 9 shows results for upsetting height of h_1 = 19 mm (Ansys).

Figure 10 shows equivalent Von Mises stress and equivalent total strain for upsetting height of h_1 = 19 mm (Msc.Marc).

Figure 11 shows results for upsetting height of h_1 = 17 mm (Ansys).

Figure 12 shows equivalent Von Mises stress and equivalent total strain for upsetting height of h_1 = 17 mm (Msc.Marc).

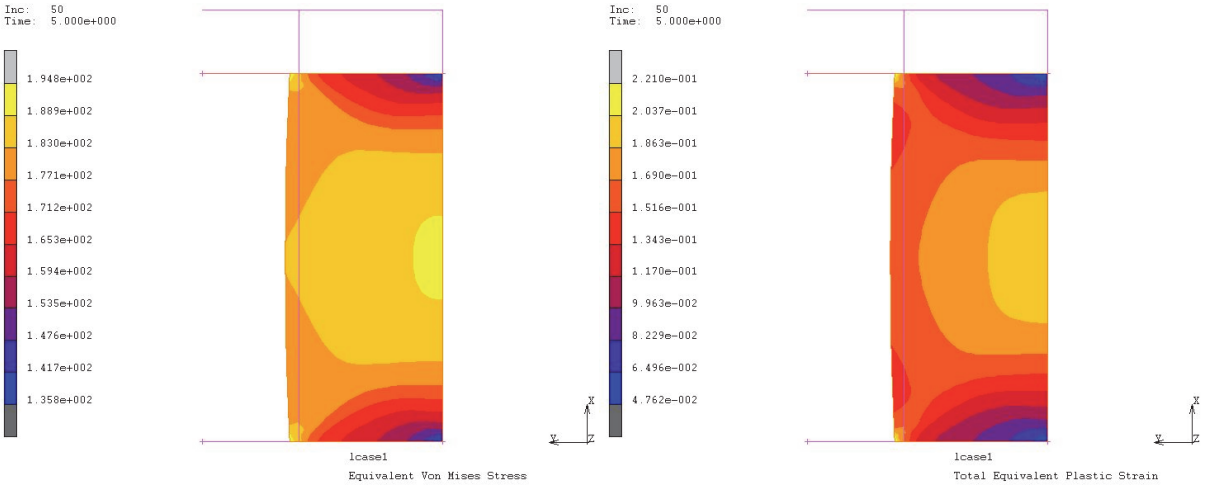

Figure 6. Von Mises stress and equivalent total strain for height of 23 mm

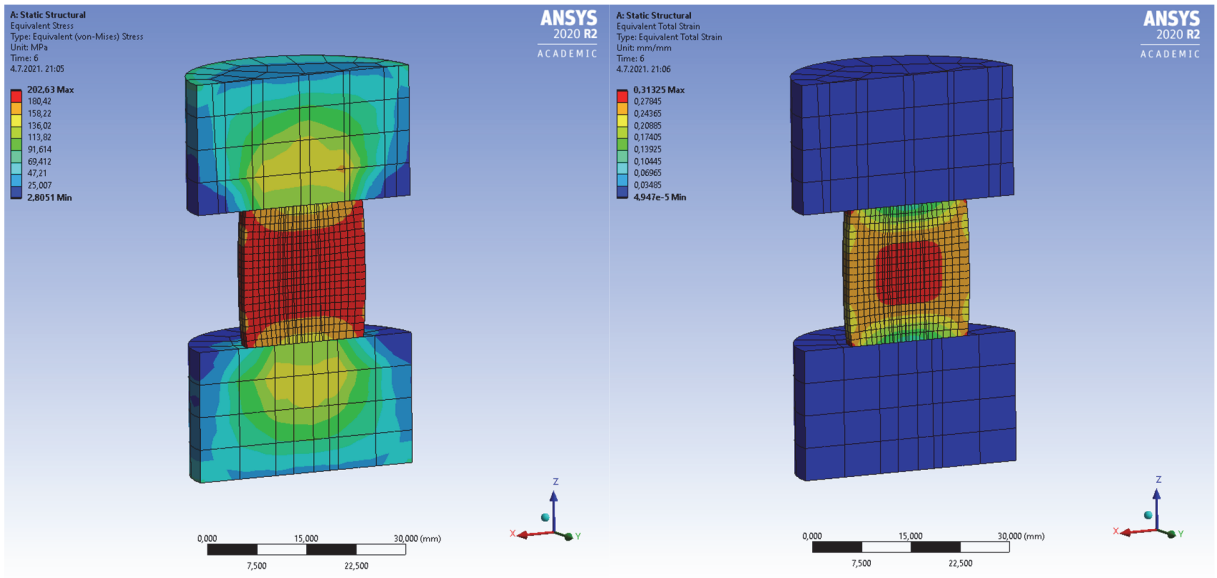

Figure 7. Von Mises stress and equivalent total strain for height of 21 mm

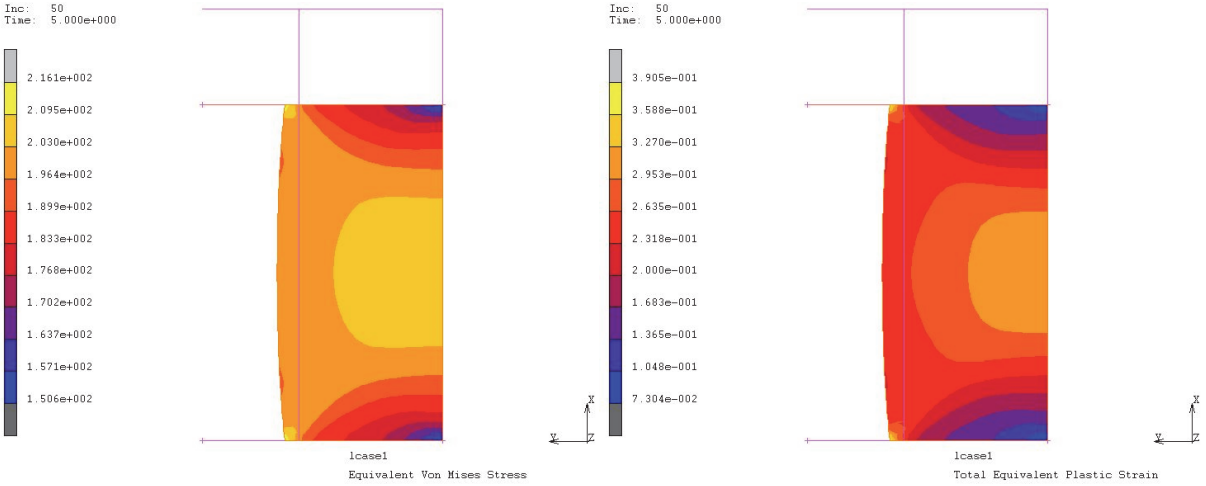

Figure 8. Von Mises stress and equivalent total strain for height of 21 mm

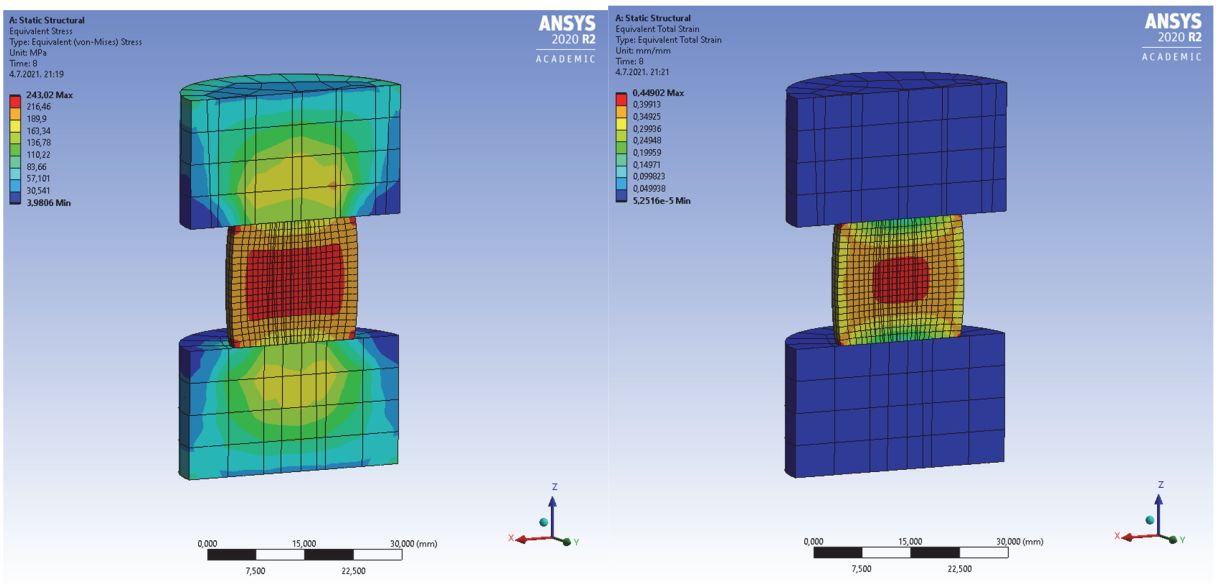

Figure 9. Von Mises stress and equivalent total strain for height of 19 mm

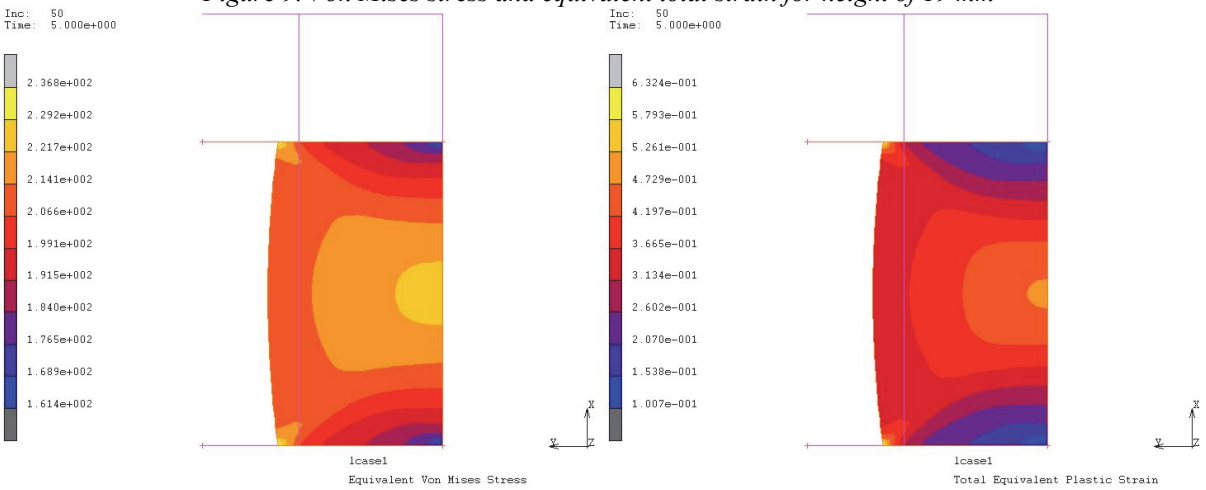

Figure 10. Von Mises stress and equivalent total strain for height of 19 mm

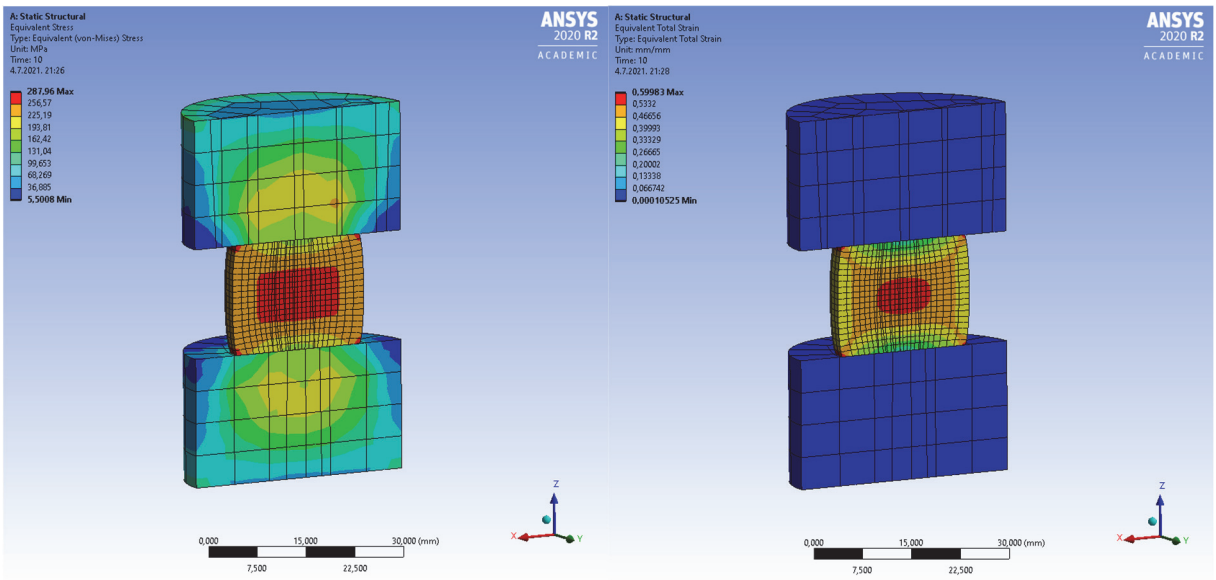

Figure 11. Von Mises stress and equivalent total strain for height of 17 mm

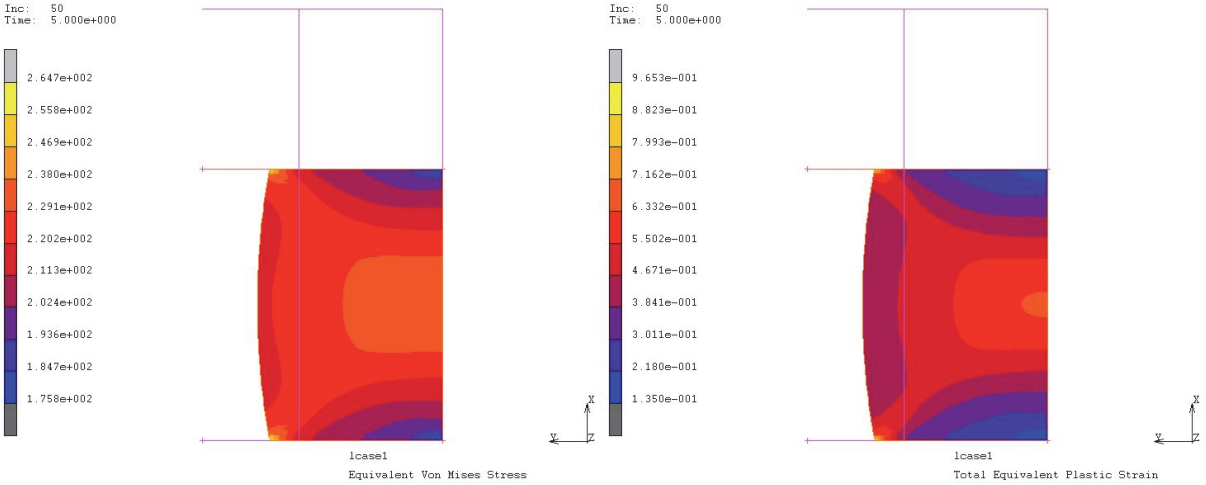

Figure 12. Von Mises stress and equivalent total strain for height of 17 mm

For the Msc.Marc different element sizes were tested (1 mm; 0,75 mm; 0,5 mm; 0,25 mm) and all had same convergence in the resulting upper tool force amount. Although it is recommended to use larger number of these elements in contact analysis [12], it has been observed that with the usage of alternative integration procedure (constant dilatation option) on mentioned element sizes – there was no adverse effect on the results. Despite there was no big difference in results, for the subsequent numerical simulations smaller element size 0,5·0,5 mm was used as per recommendation [12]. Data in table 4 shows results obtained using additive decomposition calculating procedure, data in table 5 shows results obtained using multiplicative decomposition calculating procedure.

Table 4. Results for upsetting height of 25 mm and additive decomposition calculating procedure with „assumed strain“ function enabled

No:	Element size / mm	True stress / MPa	True strain	Wall time
1.	1	157,8	0,09155	12,8
2.	0,75	157,8	0,09142	15,48
3.	0,5	157,7	0,09131	21,97
4.	0,25	157,7	0,09125	61,94

Table 5. Results for upsetting height of 25 mm and multiplicative decomposition calculating procedure

No:	Element size / mm	True stress / MPa	True strain	Wall time
1.	1	156,9	0,08926	46,86
2.	0,75	156,9	0,08907	28,62
3.	0,5	156,8	0,08898	22,5
4.	0,25	157	0,08936	162,86

Table 6. Ansys and Marc obtained dana from upsetting numerical simulations

No:	True stress / MPa	Eq. plastic strain	Force / N	True stress / MPa	Eq. plastic strain	Force / N
25	157,8	0,09131	42350	139,29	0,10016	42066
23	189,3	0,1943	55490	170,9	0,2063	55105
21	208,6	0,3242	66850	202,63	0,3125	66084
19	223,7	0,4776	79320	243,02	0,449	77663
17	237,5	0,642	94870	287,96	0,599	90163

Table 6 shows data from Ansys and Marc for conducted numerical simulations. Table 7 shows comparison of the upsetting pressure force for both numerical methods and for analytical solution.

Table 7. Comparison of calculated upsetting force

No:	Force F_1 / N (Marc)	Force F_2 / N (Ansys)	Force F_3 / N (Analytical)	ΔF_{1-3} / %	ΔF_{2-3} / %
25	42350	42066	43232,25	2,04	2,7
23	55490	55105	56282,32	1,41	2,1
21	66850	66084	67217,12	0,55	1,69
19	79320	77663	78867,72	0,57	1,53
17	94870	90163	92576,38	2,48	2,61

4 CONLUSION

Upsetting is metal forming operation where initial cylinder gets pressed in, its diameter increases and height reduces. For the ideal forming conditions this volumetric change obeys the low of incompresibillity, thus resulting area A_1 and diameter d_1 of a cylinder at the end of upsetting can be calculated. In the non-ideal conditions, friction of contact surfaces

causes friction forces, which in turn disrupt uniaxial upsetting process. After this, mathematical calculation of stress, strain and upsetting force becomes more cumbersome. For this reason the numerical methods are used to approximate those beforementioned parameters. Today there is a plethora of finite element software. Each software is based on the same theory, but they have some small differences in the element library, pre-processors, post-processors, mathematics of matrix solving etc.

In this work, finite element upsetting was numericaly modeled in Ansys and Msc.Marc. Numerical simulations were set on aluminium alloy EN AW-6060, for the cylinder of ϕ18 x 27 mm. Resulting true stresses, true strains and upsetting forces are shown, as well as the comparison between them. Overall, a good approximation of the results was obtained for both variants. Therefore, finite element method has proven as useful engineering tool where good approximation of results can be obtained very fast, opposed to cumbersome analytical (mathematical) models which are hard to apply on specialized metalforming operations.

5 REFERENCES

[1] Lange, K et. Al. Handbook of metal forming. *Society of Manufacturing Engineers*; 1st edition, January, 1995.
[2] Boljanović, V. Metal shaping processes – casting and molding, particulate processing, deformation processes and metal removal. *Industrial press*, New York, 2010.
[3] Grizelj, B. Oblikovanje metala deformiranjem/Umformtechnik/Metal forming. Strojarski fakultet u Slavonskom Brodu, Slavonski Brod, 2018.
[4] Dubois, A; Dubar, M; Dubar, L. Warm and Hot Upsetting Sliding Test: Tribology of Metal Processes at High Temperature. *Procedia Engineering Volume* 81, 2014, Pages 1964-1969.
[5] Yang, D.Y.; Choi, Y.; Kim, J.H. Analysis of upset forging of cylindrical billets considering the dissimilar frictional conditions at two flat die surfaces. *International Journal of Machine Tools and Manufacture* 31(3), 1991, Pages 397-404
[6] Priyadarshini, A; Kiran, C.P.; Suresh, K. Effect of Friction on Barreling during cold Upset Forging of Aluminium 6082 Alloy Solid cylinders. *International Conference on Recent Advances in Materials, Mechanical and Civil Engineering V330*, Hyderabad, India
[7] Aluminico. Aluminium alloy EN-AW 6060 Material data sheet. URL: https://www.aluminco.com/media/155961/ALUMINIUM-ALLOY-EN-AW-6060_MATERIAL-DATA-SHEET_ALUMINCO.pdf (8.10.2021)
[8] Nedal Aluminium BV. Alloy data sheet EN-AW 6060[AlMgSi]. URL: https://www.nedal.com/wp-content/uploads/2017/11/Nedal-alloy-Datasheet-EN-AW-6060.pdf (8.10.2021)
[9] Hydro. Technical data sheet – extruded products – alloy EN AW-6060. URL: https://www.hydro.com/Document/Index?name=Hydro%20EN%20AW%206060.PDF&id=7822 (8.10.2021).
[10] Spittel T, Spittel M. / Landolt Börstein. Numerical data and functional relationships in science and technology – Group VIII: Advanced materials and technologies. Vol 2, sub-volume C, Part 2 (Non-ferrous alloys – light metals). Springer Berlin Heidelberg New York, 2007, pp 423-429.
[11] Ngaile, G., Hiroyuki, S., Ruan, L., & Marumo, Y. A tribo-testing method for high performance cold forging lubricants. *Wear*, Volume 262, Issues 5–6, 2007, pp 684-692.
[12] Msc.Marc. Volb & MAR101. MSC software 2010.